

Robbie E. Hood<sup>1\*</sup>, Daniel Cecil<sup>2</sup>, Frank J. LaFontaine<sup>3</sup>, Richard Blakeslee<sup>1</sup>,  
Douglas Mach<sup>2</sup>, Gerald Heymsfield<sup>4</sup>, and Frank Marks, Jr.<sup>5</sup>

<sup>1</sup>NASA / Marshall Space Flight Center, Huntsville, AL

<sup>2</sup>University of Alabama in Huntsville, Huntsville, AL

<sup>3</sup>Raytheon ITSS, Huntsville, AL

<sup>4</sup>NASA / Goddard Space Flight Center, Greenbelt, MD

<sup>5</sup>NOAA Hurricane Research Division, Miami, FL

## 1. INTRODUCTION

A crucial need exists to understand and map the precipitation types, patterns, and variations of tropical cyclones (TCs) in order to develop better skill in quantitative precipitation estimation. Many efforts to identify precipitation characteristics of tropical cyclones have had extensive analysis of microwave remote sensing information.

The goal of the work presented here is to estimate precipitation type and convective intensity in TCs. An Advanced Microwave Precipitation Radiometer (AMPR) Precipitation Index (API) has been developed for an ocean surface background to produce an index value at each AMPR footprint (Table 1). In general, the API reflects the magnitude of liquid water and precipitation-sized ice aloft, based on the physical concepts of microwave rain emission and ice scattering, and is a computationally easy method to map and identify precipitation types.

## 2. INSTRUMENTATION

High resolution passive microwave brightness temperatures (TB) data from AMPR, reflectivity data from the ER-2 Doppler Radar (EDOP), and electric field data from the Lightning Instrument Package (LIP) were used here. These instruments were flown onboard the NASA ER-2 high altitude aircraft during the Third and Fourth Convection and Moisture Experiments (CAMEX-3 and CAMEX-4, 1998 and 2001). The AMPR detects passive microwave energy at 10.7, 19.35, 37.1, and 85.5 GHz. From a typical ER-2 flight altitude of ~20 km, surface footprint sizes range from 640 m (85.5 GHz) to 2.8 km (10.7 GHz). The EDOP operates at 9.6 GHz and provides high resolution time-height sections of reflectivity and hydrometeor vertical velocity. The LIP provides full vector components of the atmospheric electric field.

## 3. DEVELOPMENT

For each AMPR scan, the API of the two nadir pixels is collocated with the simultaneous nadir reflectivity profile from EDOP. A characteristic (median) EDOP reflectivity profile is then assigned to each API. Any variability about each characteristic profile is assessed using the cumulative density function (CDF) of reflectivity. It is

theorized the API can be applied to various problems after converting to rain rate or ice mass. This can be accomplished with a Z-R or other suitable relationship for a particular application. Finally, electric fields and API are plotted together on the aircraft track to assess electrical activity, or lack thereof, with convective intensity.

The API and the LIP fields are projected onto the aircraft track over Hurricane Bonnie on 26 Aug 1998 (1500-1600 UTC; Fig. 1). Consider the SE-NW overpass and the vertical cross-section of reflectivity from EDOP (Fig. 2). There is very good agreement with the API, the electric fields, and the radar reflectivity. As expected, the technique has some trouble with detecting thinner cirrus.

Based on comparison with radar data, the technique shows promise as a high spatial and temporal resolution precipitation identification and mapping tool. Matching the rainfall classification results with coincident electric field information collected by LIP readily identifies highly convective rain regions within TC precipitation fields. Further study may quantify the relationship between lightning and microwave information as a surrogate indicator of convective strength. More extensive examination using NOAA P-3 radar and the CAMEX microphysical data will be conducted to explore the feasibility of adding a rain rate conversion algorithm to the API technique for use as a quantitative precipitation estimation tool.

## 4. DISCUSSION

This technique shows promise as a real-time analysis tool for monitoring precipitation, vertical updraft strength, and convective intensity from traditional aircraft or uninhabited aerial vehicles (UAVs). The synergy of the AMPR, EDOP, and LIP data sets has been presented here not only as a research tool for those interested in hurricane studies or as a validation tool for those developing satellite rainfall algorithms, but also as an example of how airborne information may be merged into real-time observational products. Future concepts for Earth observation include adding airborne platforms such as uninhabited aerial vehicles or ultra-long duration balloons into a mixture of spaceborne and surface-based assets comprising a flexible, adaptive global observation network. Within these types of frameworks, an airborne vehicle could be positioned to provide high spatial and temporal resolution coverage of a critical weather event in concert with spaceborne and

---

\*Corresponding Author: Robbie E. Hood, Earth Science Department (Code SD60), NASA Marshall Space Flight Center, Huntsville, AL 35812; Robbie.Hood@nasa.gov

surface instrumentation so that the best combination of information is used for observation and prediction of the event outcome. As technical development of airborne platforms for this type of use progresses, appropriate airborne instrumentation and data algorithms should be identified that provide the maximum amount of information using the most feasible airborne payload for a given application. This study presents instrument candidates that could be used for high altitude monitoring of precipitation type and convective strength for tropical cyclone and other precipitation systems. The research and operational communities should also examine many other types of instruments and flight altitudes in order to choose the optimal mixture of observations.

## 5. REFERENCES

Heymtsfield, G.M., J.B. Halverson, J. Simpson, L. Tian, and T.P. Bui, 2001: ER-2 Doppler radar investigations of

the eyewall of Hurricane Bonnie during CAMEX-3. *J. Appl. Meteor.*, 40, 1310-1330.

Mach, D. M., and W. J. Koshak, General matrix inversion technique for the calibration of electric field sensor arrays on aircraft platforms, Preprints, 12th Int. Conf. on Atmos. Electr., June 2003.

Spencer, R.W., R.E. Hood, F.J. LaFontaine, E.A. Smith, et al., 1994: High resolution imaging of rain systems with the Advanced Microwave Precipitation Radiometer. *J. Atmos. Oceanic Technol.*, 11, 849-857.

### Acknowledgement

Dr. Ramesh Kakar, NASA Headquarters Atmospheric Dynamics and Remote Sensing Program Manager, funded this work through CAMEX NASA Research Announcement (NRA-00-OES-06).

Table 1: The API matrix with the indices, cloud, rain, and ice levels cross-referenced by color. Cloud level categories are non-precipitating. Ice and cloud level 0 does not necessarily indicate a zero quantity.

| ICE LEVELS | CLOUD LEVELS |   |   | RAIN LEVELS |          |          |         |          |    | API |       |
|------------|--------------|---|---|-------------|----------|----------|---------|----------|----|-----|-------|
|            | 0            | 1 | 2 | 1           | 2        | 3        | 4       | 5        | 6  |     |       |
| 0          |              |   |   |             |          |          |         |          |    |     | 0-5   |
| 1          |              |   |   |             |          |          |         |          |    |     | 6-10  |
| 2          |              |   |   |             |          |          |         |          |    |     | 11-15 |
| 3          |              |   |   |             |          |          |         |          |    |     | 16-18 |
| API        | 0            | 1 | 2 | 3, 6, 11    | 4, 7, 12 | 5, 8, 13 | 9,14,16 | 10,15,17 | 18 | API |       |

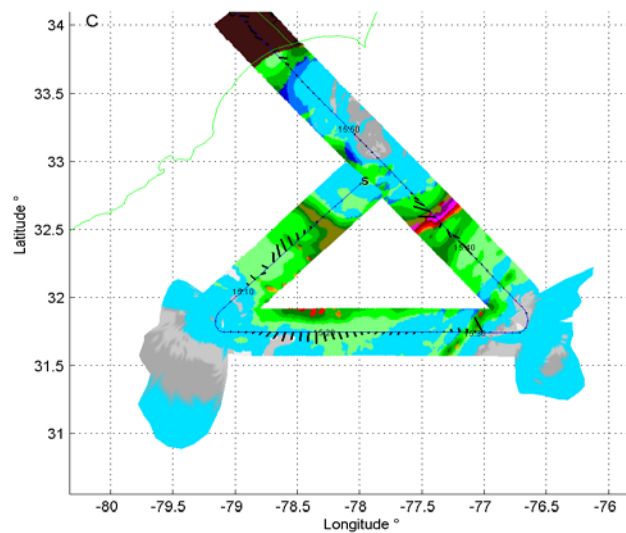


Figure 1. Shown is the API and horizontal electric field to the x-y plane. Electric field ( $10^4$ V/m<sup>2</sup>) bars are plotted originating at the aircraft location. Refer to Table 1 for API color codes and meanings.

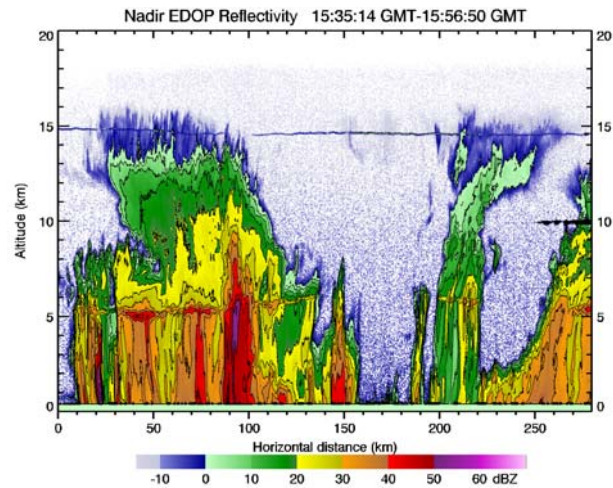


Figure 2. Vertical cross-section of nadir EDOP reflectivity, 1535 – 1557 UTC 26 Aug 1998. Cross-section extends from 170 km southeast of the center of Hurricane Bonnie (left) to 110 km northwest of the center (right).